Eddy Current Loss Estimation of Edge Burr affected Magnetic Laminations Based on Equivalent Electrical Network-Part I Fundamental Concepts and FEM Modeling

Hamed Hamzehbahmani[1], Phil Anderson[1], Jeremy Hall[1] and David Fox[2]
[1]Wolfson Centre for Magnetics, Cardiff University, Cardiff CF24 3AA, UK
[2]Cogent Power Ltd., Newport NP19 0RB, UK

***Abstract*— Cutting and punching of the electrical steels can cause edge burrs which lead to inter-laminar short circuits between the laminations. In this work based on equivalent electric circuit of the eddy current path, an analytical method has been developed to estimate the eddy current power loss of the magnetic cores, caused by the inter-laminar faults, in a wide range of flux density and magnetising frequency. Important factors such as skin effect, non-uniform flux density distribution, complex relative permeability and non-linear relation of *B (H)*, which are often neglected in the literature, are highlighted. Fundamental concepts of inter-laminar fault and its consequences, effect of inter-laminar faults on configuration of magnetic cores and FEM verification are presented in this Part I paper. Modeling of eddy current together with experimental results of eddy current measurements of packs of shorted laminations are reported in Part II.**

Keywords: eddy current power loss, edge burr, inter-laminar fault, skin effect, complex relative permeability, high frequencies, FEM modeling.

1. INTRODUCTION

MAGNETIC cores of electrical machines are constructed from laminations of magnetic steel core material alloyed with silicon to minimize the hysteresis and eddy current losses for high efficiency operation [1]. Since the magnetic cores are exposed to time-varying magnetic fields, eddy currents are induced in the laminations and consequently, energy is converted into heat in the resistance of the eddy current path. The laminations are coated with insulation material on either side to prevent electrical conduction between the sheets. However punching and cutting of the electrical steels to the required dimensions can cause edge burrs which are one of the most serious obstacles to precision manufacturing and manufacturing processes automation [2-5]. Burrs are formed in various machining process as a result of plastic deformation during mechanical manufacturing processes, e.g. cutting and punching, and have to be removed by a deburring process for functional and technical reasons after the workpiece is machined. The cut and punch edge shall not exceed 0.05 mm on a length of lamination strip of 10 mm. Punctual edges are allowed up to 0.1 mm [6]. In some design of electrical machine, high surface insulation resistance is a major requirement and a thick coating is normally used to ensure short circuits arising from burrs are not problematical [7]. However particular coating or adding a deburring process means extra cost, extra manufacturing time, and an extra machining station [8]. Since burr generation in machining cannot be avoided completely, it is necessary to study their effects and consequences on the magnetic and electrical properties of electrical machines.

Edge burrs could lead to short circuits between adjacent laminations. However, if edge burrs appear between two sheets of the magnetic core on one side only, it does not create a closed current path and no change in the total iron loss of the core occurs. But, if the same two sheets are short-circuited on both sides, a closed conductive path will be available which leads to a larger section for the flow of inter-laminar eddy currents which results in elevated eddy current loss [9]. Fig 1-a shows a 3-D view of a transformer limb with an inter-laminar fault in the top step. Eddy current in laminations without fault and inter-laminar eddy currents in the presence of the fault, from the cross section view of Fig 1-a, are shown in Figs 1-b and 1-c, respectively.

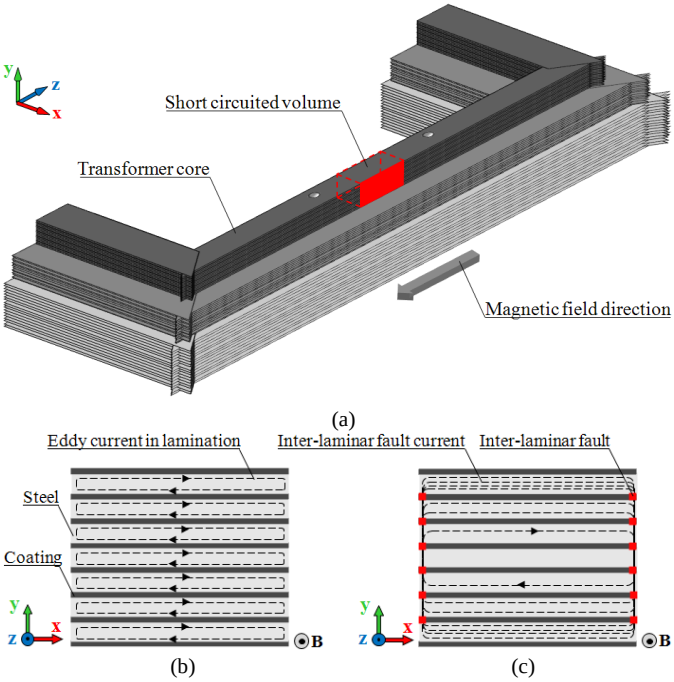

Fig 1 (a) 3-D view of a transformer limb with inter-laminar short in the top step (b) Eddy current path in the laminations without inter-laminar fault (c) Inter-laminar eddy current path with inter-laminar fault

A few shorts between the laminations may not create a high inter-laminar eddy current; but with several shorts on either side of the core the induced inter-laminar eddy currents could be large and cause excessive local heating in the damaged area

[10]. If the generated heat cannot be dissipated adequately, it can cause more inter-laminar failures and may eventually cause burning or melting the iron core and thus it raises the potential of a complete machine failure [10-17]. Localised heating due to the inter-laminar fault currents can also damage the excitation winding insulation and lead to ground failure [1]. Two examples of core melting caused by inter-laminar insulation failure are shown in Fig 2 [1] and [10].

(a) (b)

Fig. 2 Stator core melting caused by inter-laminar insulation failure (a) core fault in tooth wall [1] (b) core fault in tooth bottom [10]

In this Part I paper, the fundamental concepts of an inter-laminar fault and its consequences on magnetic cores are discussed. Effect of inter-laminar fault on configuration of laminations and eddy current distribution of the magnetic cores in a wide range of frequency by focusing on the skin effect are presented. Finally FEM verification and flux density distribution along the equivalent configuration of magnetic cores with inter-laminar fault are presented.

2. Nature of the Eddy Current and the Eddy Current Power Loss

When a time-varying magnetic field is applied to a conducting material, an *emf* is induced in the material, in accordance with *Faraday's law of induction*. Considering the electrical conductivity of the material, the induced *emf* along a closed path inside the material sets up a current along that path to circulate and penetrate conducting parts. The direction of the eddy current is perpendicular to the direction of the magnetic field, while the distribution pattern depends on the shape of the conductor. Fig 3 shows the induced eddy current for cubic and cylindrical shape conducting materials. Regardless of the driving force, the eddy current density is found to be greatest at the conductor's surface, with a reduced magnitude deeper in the conductor.

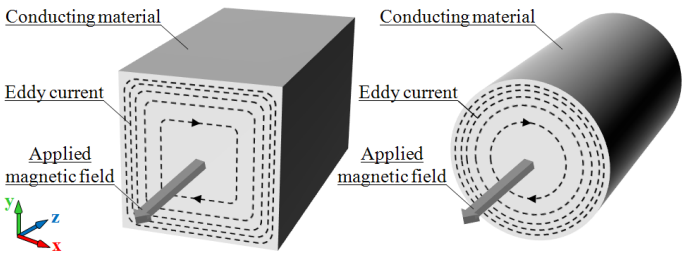

(a) (b)

Fig 3 Induced eddy current in conducting materials exposed to time-varying magnetic field

That decline in current density is known as the *skin effect* and *depth of penetration* or *skin depth* is a measure of the depth at which the current density falls to e^{-1} (approximately 0.367) of its value near the surface [18]. The skin depth δ of any conducting material is defined by:

$$\delta = \sqrt{\frac{2}{\omega\mu\sigma}} = \frac{1}{\sqrt{\pi f \mu\sigma}} \quad (1)$$

Where f [Hz], μ [H/m] and σ [S/m] are frequency, absolute magnetic permeability and electrical conductivity of the material, respectively. From equation (1), for each material with given permeability and conductivity the penetration of the eddy current, which is quantified by skin depth, is highly frequency dependent. For conductors with small relative diameter and low operating frequency, skin effect might be negligible. However at higher frequencies, where the skin depth is smaller, the effective cross-section is reduced and hence the effective resistance of the conductor is increased and it affects the characteristics of the conductor. Therefore skin depth is a determinant parameter in eddy current modeling and estimation, especially at high frequencies.

Eddy currents, and hence eddy current power loss, are minimised in the magnetic devices by using thin sheets of magnetic material, known as laminations. Laminating the magnetic cores can reduce the skin effect, at low frequencies, as well. At high frequencies skin effect is an important factor and should be taken into account in accurate modeling of the eddy current loss. However, in a burr affected magnetic core, skin effect might become significant even at low frequencies.

3. Flux Density Distribution Inside Single Sheet Magnetic Lamination

One of the major factors in eddy current power loss determination is the magnetic flux density distribution along the thickness of the lamination which depends on magnetising frequency. Fig 4 shows a 3-D view of a single sheet lamination of thickness $t=2a$ in a time-varying magnetic field $B_s \cos \omega t$ (B_s: flux density at surface) applied in the rolling direction.

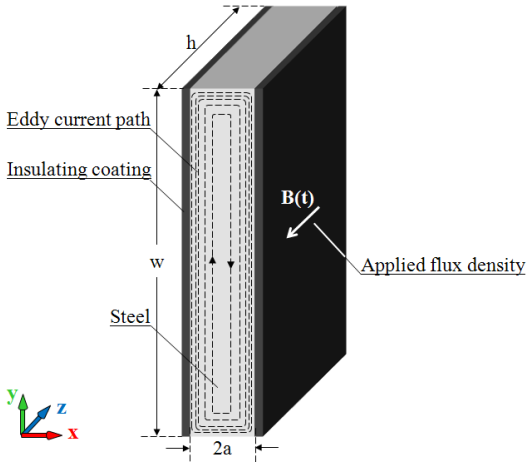

Fig 4 3-D view of a magnetic lamination of thickness *2a* under time-varying magnetic field ***B****(t)*

In this figure, z and y directions represent rolling and transverse (90° to the direction of rolling) directions of the lamination, respectively. If eddy current loops are assumed to be large enough along the transverse direction, the field problem becomes one dimensional and can be reduced to a single equation for z-component of magnetic flux density $B_z(x,t)$ that depends on x and t [19]:

$$\frac{\partial^2 B_z(x,t)}{\partial x^2} = \mu_0 \mu_z \sigma \frac{\partial B_z(x,t)}{\partial t} \quad (2)$$

where μ_z is permeability of the material at a particular flux density B_z. Equation (2) is a differential equation which defines the flux density B_z as a function of distance x and time t and has the value $B_s \cos \omega t$ when x is $\pm a$. This equation was solved for a particular relative permeability and magnetic flux density based on the method stated in [19]; therefore the instantaneous flux density at any point inside the lamination is obtained by:

$$B_z(x,t) = B_s \sqrt{\frac{\left(\cosh \frac{2x}{\delta} + \cos \frac{2x}{\delta}\right)}{\left(\cosh \frac{2a}{\delta} + \cos \frac{2a}{\delta}\right)}} \cos(\omega t - \beta) \quad (3)$$

Where δ is skin depth, which was defined by equation (1) and β is the phase angle of the flux density and can be obtained by:

$$\tan \beta = \frac{\sinh p(a-x) \sin p(a+x) + \sinh p(a+x) \sin p(a-x)}{\cosh p(a-x) \cos p(a+x) + \cosh p(a+x) \cos p(a-x)} \quad (4)$$

Where $p=1/\delta$. Equation (3) defines flux density along the thickness of the lamination as a function of distance x from the centre line of the lamination, skin depth δ and time t. Substituting $x=\pm a$ into (3), the flux density at the surface of the lamination is obtained as equation (5):

$$B_z(a,t) = B_z(-a,t) = B_s \cos \omega t \quad (5)$$

3.1. Flux density dependence of the relative permeability

In order to extend the solution of (2) to a wide range of flux density, non-linear relation of $B(H)$ was taken into account by measuring the relative permeability of the material. Neglecting flux leakage around the magnetic core, effective relative permeability μ_r as a function of magnetic flux density can be obtained using the following equation [20]:

$$\mu_r = \frac{B_{pk} l_m}{\mu_0 N I_{pk}} \quad (6)$$

Where B_{pk} is peak values of magnetic flux density, l_m is mean magnetic path length of the magnetic circuit, μ_0 is permeability of free space, N is number of turns of the magnetising coil and I_{pk} is measured peak magnetising current. Based on (6), the relative permeability of a single sheet lamination of CGO at flux densities 0.1 T to 1.8 T and 50 Hz frequency was measured using a single sheet tester (SST); the result is shown in Fig 5. As shown in in this figure, relative permeability of the magnetic laminations varies significantly with flux density. To increase the accuracy of the analytical model, this variation should be considered in calculating of eddy current power loss and other magnetic quantities.

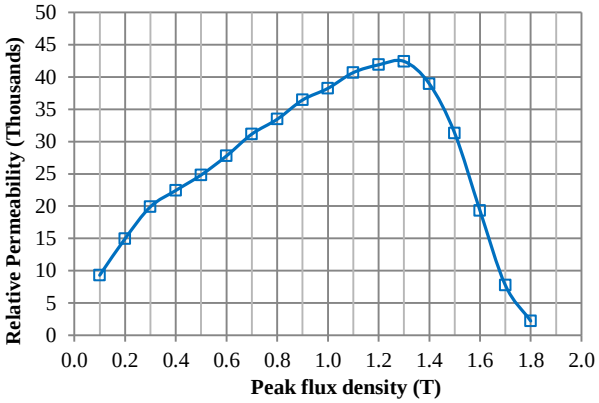

Fig 5 Flux density dependence of the effective relative permeability of CGO at magnetising frequency 50 Hz

3.2. Complex relative permeability at high frequencies

Due to the inductive nature of the magnetic materials, there is a time lag between magnetic flux density $\boldsymbol{B}$ and magnetic field strength $\boldsymbol{H}$. However at low frequencies this time lag is negligible but at high frequencies it might be significant and should be taken into account. To analyse these phenomena in magnetic cores, it is convenient to consider the relative magnetic permeability of the material as the complex quantity $\mu_r = \mu_r' - j\mu_r''$ in which μ_r' and μ_r'' are real functions of the magnetising frequency f [21]. The effective relative complex permeability of the lamination in the rolling direction can be obtained by [21]:

$$\mu_z^{eff} = \mu_z' - j\mu_z'' = \mu_z \frac{\tanh(a\gamma)}{a\gamma} \quad (7)$$

Where μ_z is the absolute static permeability of the material in the rolling direction and γ is propagation constant which is directly related to the the skin depth δ by [21]:

$$\gamma = \frac{(1+j)}{2\delta} \quad (8)$$

Real and imaginary parts of the effective complex permeability as a function of the magnetising frequency are shown in Fig 6. The computations of Fig 6 were performed using the following parameters for 3 % grain oriented silicon steel material: thickness=0.3 mm, conductivity, $\sigma=2.17\times10^6$ S/m (measured based on the method in [22]) relative permeability, $\mu_z=3.13\times10^4$ at peak flux density of 1.5 T (derived from Fig 5).

A flowchart was designed to calculate magnetic flux density distribution along the lamination thickness at each frequency and flux density, as shown in Fig 7. According to the designed flowchart, the magnetising frequency and amplitude of the flux density are initially set at the required values. Relative permeability μ_r at the specific flux density is then read from the measured values of Fig 5. Complex relative permeability of the

material will be then calculated using equation (7); and finally, local flux density B_x at the specific values of magnetising frequency and amplitude of surface flux density will be calculated using equation (3).

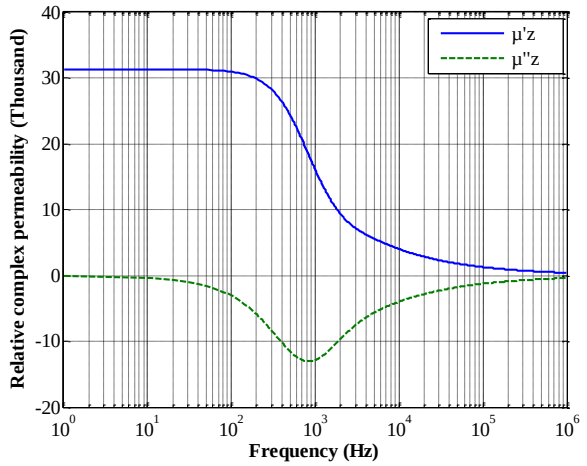

Fig 6 Real and imaginary parts of relative complex permeability of a single strip magnetic lamination in rolling direction at peak flux density of 1.5 T

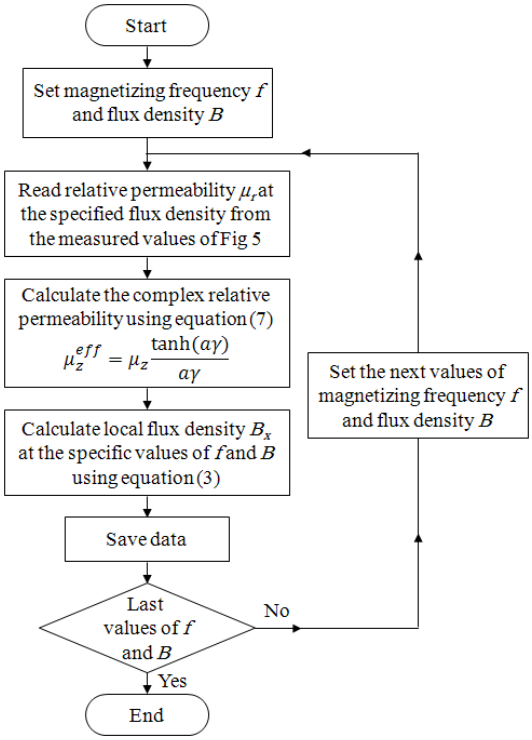

Fig 7 Flowchart of calculation of the flux density distribution

Based on the design flowchart, magnetic flux density distribution (normalized by the value at the surface) along the thickness of the lamination for different values of the magnetising frequency f and particular surface flux densities 1.3 T and 1.7 T are shown in Fig 8. These curves were obtained by the following parameter values for 3% GO silicon steel with thickness of 0.3 mm: σ=2.17×10^6 S/m and μ_r=4.24×10^4 at 1.3 T and μ_r=7.75×10^3 at 1.7 T.

Two important notes could be taken from Fig 8. The first note is related to flux density distribution along the lamination thickness. From equation (3), half of the lamination thickness, a, and skin depth, δ, are two determinant factors in the qualification of the flux density distribution along the lamination thickness. At low frequencies, where $\delta>>a$, flux density distributes uniformly along the lamination thickness. However, at high frequencies where $\delta<<a$, the flux density at the centre region of the lamination is nearly zero, and corresponding high flux density is noted near the surfaces of the lamination. And secondly, Fig 8 shows that flux density distribution along the lamination thickness not only depends on magnetising frequency but also depends on peak magnetic flux density which is related to the non-linear relation of *B (H)*.

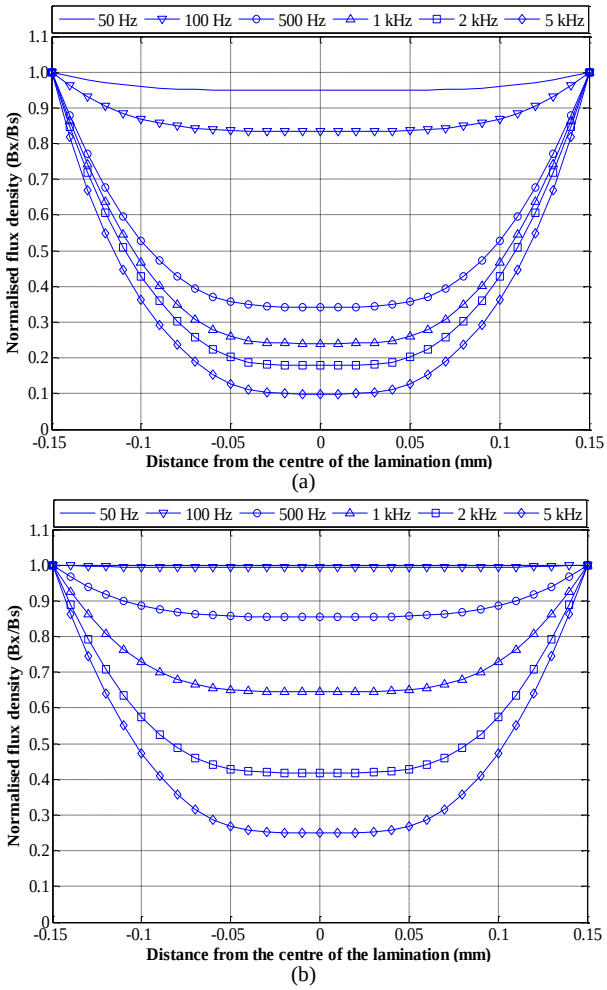

Fig 8 Normalized magnetic flux density penetration into magnetic lamination of thickness $2a$=0.3mm at different frequencies (a) B_s=1.3 T (b) B_s=1.7 T

From equation (1) at a specific frequency, the only parameter that could vary with flux density is the relative permeability of the material which in turn could affect the flux density penetration. In order to investigate this phenomenon, variation of the skin depth of CGO material was calculated at magnetising frequencies of 50 Hz, 100 Hz and 500 Hz and flux density from 1.0 T to 1.8 T; the results are shown in Fig 9. This figure shows significant skin effect at low flux densities; however this effect becomes negligible at high flux densities. These fluctuations are related to the effect of flux density on the relative permeability or non-linear relation of *B (H)*.

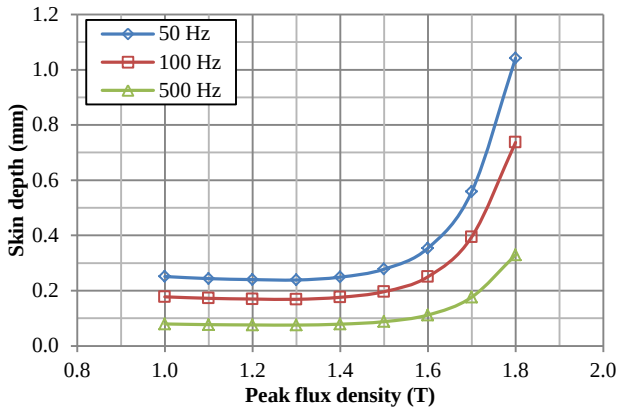

Fig 9 Effect of flux density on skin depth for CGO material at magnetising frequencies 50 Hz, 100 Hz and 500 Hz

4. EFFECT OF INTER-LAMINAR FAULT ON THE CONFIGURATION OF THE MAGNETIC CORES

In a perfectly assembled core, when the laminations are well insulated from each other, the eddy current paths are restricted to individual laminations, as shown in Fig 1-b. This is due to the insulation coating on the surface of the steel preventing electrical connection between adjacent laminations [5]. The primary hypothesis about the effect of the edge burr on the magnetic cores is to change the configuration of the burred laminations to a solid core with equivalent thickness of *2na*, where *n* is number of the adjacent burred laminations and *a* is half of the thickness of one lamination.This hypothesis for packs of two and three laminations is illustrated in Fig 10.

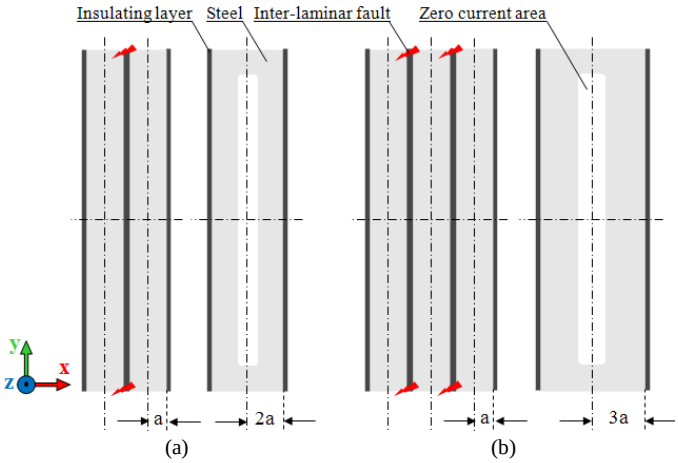

Fig 10 Cross section area of (a) two and (b) three magnetic laminations of thickness *2a* with short circuit on either sides and equivalent configurations

4.1. FEM verification

In order to verify this hypothesis, 2-D FEM simulations for stacks of two, three and five laminates were performed using COMSOL Multiphysics. Fig 11 shows the FEM mesh model for the upper end above of the line of symmetry of a stack of five laminations with inter-laminar short. Each lamination has a thickness of 0.3 mm and they are separated by an air gap of 20 µm. The laminations were exposed to a time-varying outward magnetic field (Out of the page). As the first part of this investigation, the laminations were magnetised without inter-laminar fault and with inter-laminar fault on one side only. The result of this investigation at magnetising frequency of 50 Hz is shown in Figs 12-a and 12-b, respectively.

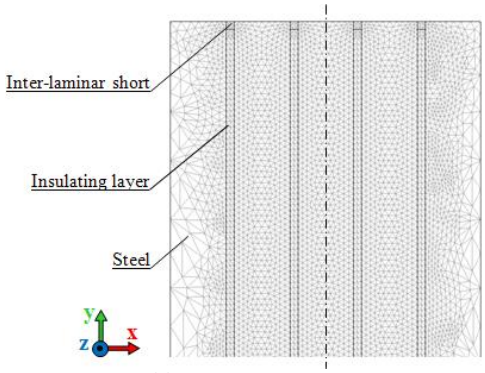

Fig 11 FEM mesh model of five laminations with inter-laminar short circuit

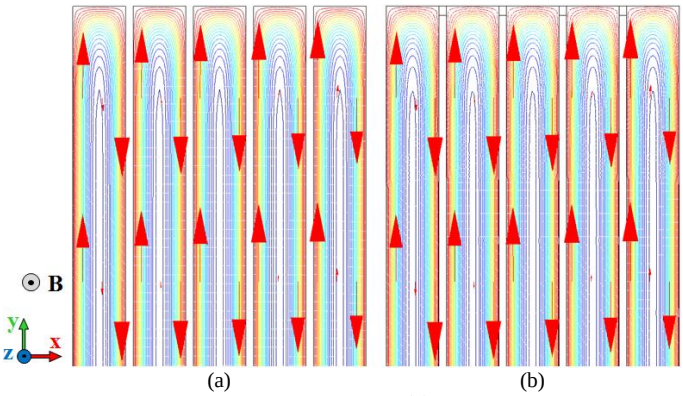

Fig 12 Eddy current distribution in a stack of five laminations (a) without inter-laminar fault (b) with inter-laminar fault on one side only; at 50 Hz

Fig 12-a shows the ideal performance of magnetic cores, i.e. without inter-laminar fault between the laminations, in which eddy currents are restricted to individual laminations. On the other hand, as expected initially, eddy currents at the shorted end of Fig 12-b are still restricted to the individual laminations. Inter-laminar eddy current between the laminations requires a closed path perpendicular to the flux density in the core. Therefore, as shown in Fig 12-b, if edge burrs appear between the laminations of the magnetic core on one side only, it does not create a closed current path and no change in the eddy current distribution and hence eddy current power loss occurs.

Magnetic laminations were then shorted together on either side. Eddy current distribution in the cores with two, three and five laminations with inter-laminar fault on both sides at magnetising frequencies of 50 Hz and 1000 Hz are shown in Figs 13 and 14, respectively. Due to the known symmetry in the *y*-direction, only one end of the laminations is shown.

Five important points could be concluded from the FEM results of Figs 12 and 13:

1. There is only one eddy current loop in each pack of the shorted laminations; which can prove the primary hypothesis.
2. The inter-laminar faults change the configuration of the magnetic cores to be similar to a solid core which leads to inter-laminar fault current and larger eddy current loops.
3. Eddy current density at the shorted ends is much higher than the laminations which lead to local power loss at the shorted ends.

4. Changing the configuration of the burred laminations causes skin effect to become significant, even at low frequencies.

5. The equivalent configuration which is affected by the skin effect leads to a zero current area at the centre line of the equivalent configuration. The position and width of the zero current area in the equivalent configurations depends on number of the shorted laminations, magnetising frequency and flux density.

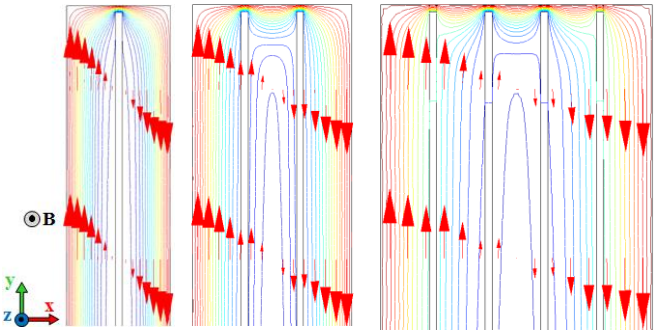

(a) (b) (c)

Fig 13 2-D FEM modeling of eddy current distribution in burr affected magnetic laminations at magnetising frequency of 50 Hz
(a) two (b) three and (c) five laminations

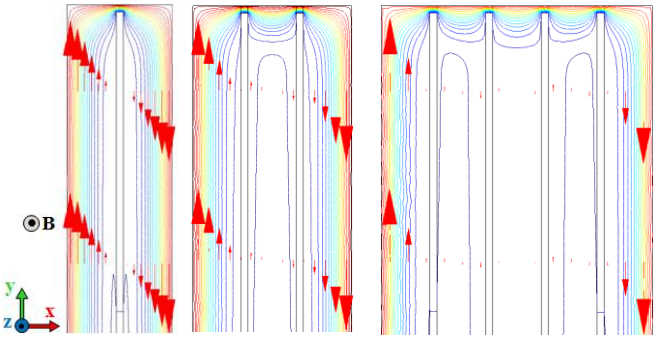

(a) (b) (c)

Fig 14 2-D FEM modeling of eddy current distribution in burr affected magnetic laminations at magnetising frequency of 1000 Hz
(a) two (b) three and (c) five laminations

In order to visualize eddy current distribution along the shorted laminations, the FEM results of induced eddy current density normalized by surface value for packs of two, three and five shorted laminations at magnetising frequencies of 50 Hz and 1000 Hz are shown in Figs 15-a and 15-b, respectively.

Fig 15 shows that regardless of the gaps between the shorted laminations, the induced eddy currents in the laminations at 50 Hz are a linear function of distance from the centre line, but not at 1000 Hz. It will be discussed further in section 2.1 of Part II paper based on the induced voltage in the magnetised lamination. However, these curves emphasise the importance of skin effect on magnetic properties of burred laminations. Therefore to investigate the effect of inter-laminar fault on the magnetic properties of the magnetic cores, shorted laminations can be modeled by a solid core with equivalent thickness of *2na*. However as demonstrated by the FEM modeling, in presence of inter-laminar fault skin effect becomes significant, even at low frequencies, and should be taken into account in the related studies.

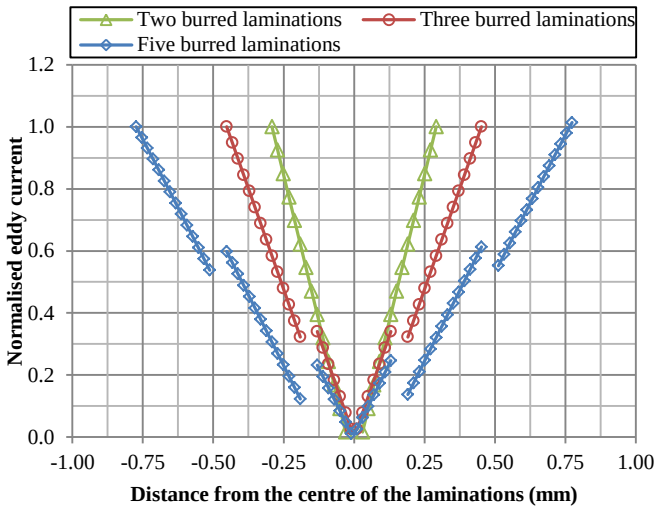

(a)

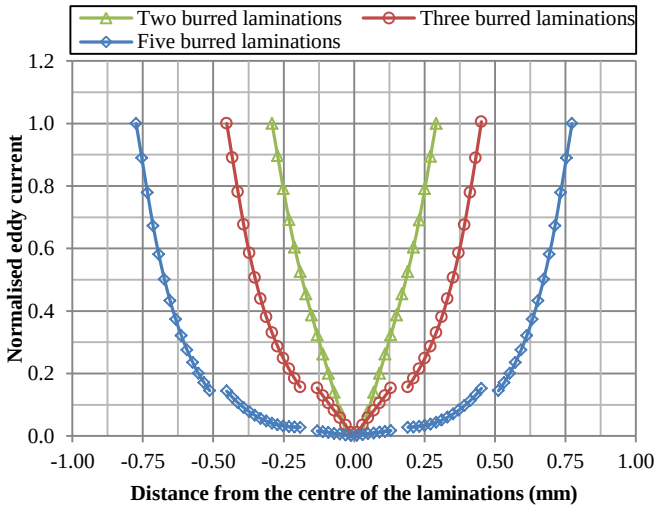

(b)

Fig 15 FEM result of normalized induced eddy current density in packs of two, three and five laminations at frequencies (a) 50 Hz (b) 1000 Hz

4.2. Flux density distribution in burred laminations

From equation (3), half of the lamination thickness, *a*, and skin depth, *δ*, are two determinant factors in the qualification of the flux density distribution along the lamination thickness. In time-harmonic investigations it is usual to compare the thickness or diameter of the cross section of the conducting materials with the equivalent skin depth at each particular operating point. Therefore it is useful to compare the ratio of half of the lamination thickness to the skin depth (*a/δ*) for different thicknesses, flux densities and magnetising frequencies. Fig 16 shows *a/δ* ratio versus flux density for different lamination thicknesses at magnetising frequency of 50 Hz. The curves of a=0.15 mm indicate *a/δ* ratio versus flux density of single strip lamination and the curves of a=0.3 mm, a=0.45 mm, a=0.6 mm and a=0.75 mm are equal to those of the packs of two, three, four and five shorted laminations, respectively.

Fig 16 shows that for a single lamination with a=0.15 mm (thickness of 0.3 mm) at 50 Hz frequency, *a/δ*<1 for all flux

densities. Therefore in this case skin effect can be neglected and flux density distributes almost uniformly along the lamination thickness, as shown in Fig 8. However since skin depth δ is a constant value at a given frequency and flux density, by increasing the thickness of the lamination it will become significant; i.e. the a/δ ratio becomes greater than unity even at low frequency. Therefore considering the effect of the edge burrs on the configuration of the burred laminations, significant skin effect and non-uniform flux density distribution along the equivalent thickness of the burred laminations are expected, even at low frequencies.

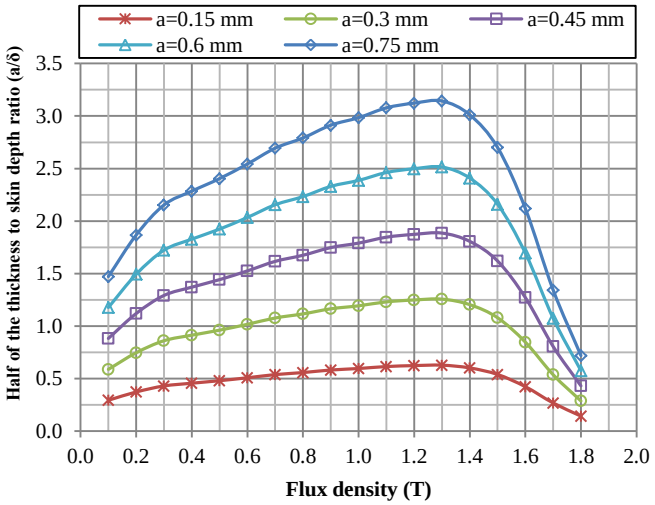

Fig 16 Half of the thickness to skin depth ratio (a/δ) versus flux density at different thickness at frequency 50 Hz

From equations (7) and (8), skin effect δ and half of the lamination thickness a are also two key factors in complex relative permeability. Therefore inter-laminar short circuits also affect the complex relative permeability of the material. Amplitude and phase angle of the complex relative permeability of the material with the specifications given in section 3 typically at surface flux density B_s=1.5 T for five different thicknesses, a=0.15 mm to a=0.75 mm, are shown in Fig 17. The amplitude of the complex relative permeability decreases by increasing the magnetising frequency. However in the presence of inter-laminar faults, which lead to an increase of the effective thickness of the damaged laminations, the amplitude of the complex relative permeability is reduced at lower frequencies, i.e. for laminations of 0.3 mm thickness complex relative permeability is constant up to about 100 Hz while for the lamination of 1.5 mm thickness it drops at a few Hertz. Therefore, in presence of the inter-laminar fault the complex relative permeability becomes more significant and should be taken into account, even at low frequencies.

Using the designed flowchart of Fig 7 normalized flux density distributions along the lamination thickness at surface flux densities 1.3 T and 1.7 T and magnetising frequency of 50 Hz for different thicknesses of the lamination from 0.3 mm to 1.5 mm are shown in Fig 18. In these curves non-linear relation of *B (H)* and complex relative permeability of Fig 17 were taken into account. The results presented in Fig 18 show that at 50 Hz flux density is distributed almost uniformly along the lamination with a thickness of 0.3 mm; however by increasing the lamination thickness, at the same flux density and magnetising frequency, half of the thickness a will become greater than the skin depth δ and therefore flux density drops from the edge of lamination to the centre line.

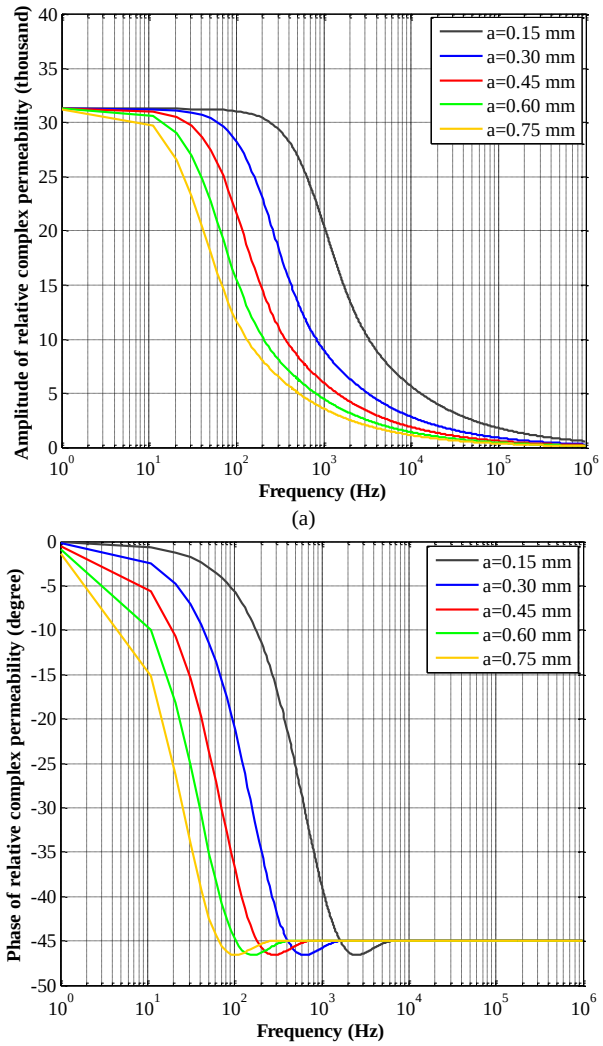

Fig 17 Frequency dependence of (a) amplitude and (b) phase of the relative complex permeability of a magnetic lamination in rolling direction for different lamination thicknesses at B_s=1.5 T

Therefore, it can be concluded that the importance of the skin effect on the eddy current distribution and eddy current power loss is not only at high frequencies, but also at low frequencies when the core is affected by inter-laminar faults.

5. Conclusion

In this Part I paper fundamental concepts of inter-laminar fault and its consequences on the magnetic cores were presented. An equivalent configuration was proposed for magnetic cores with inter-laminar faults. 2-D FEM modeling was performed to verify the equivalent configuration and visualize eddy current paths in along the lamination thickness.

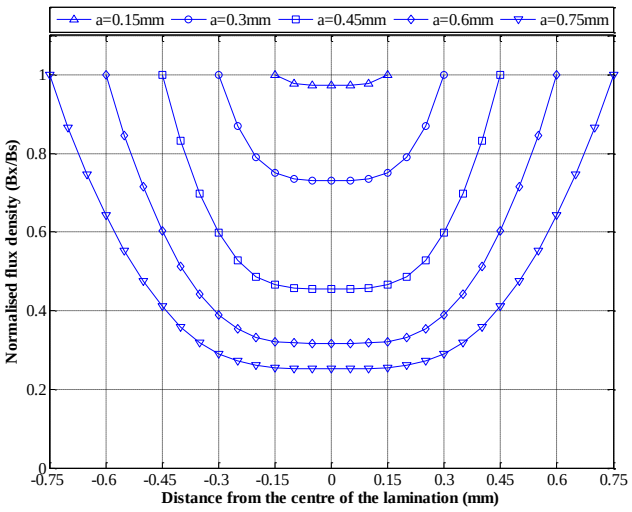

(a)

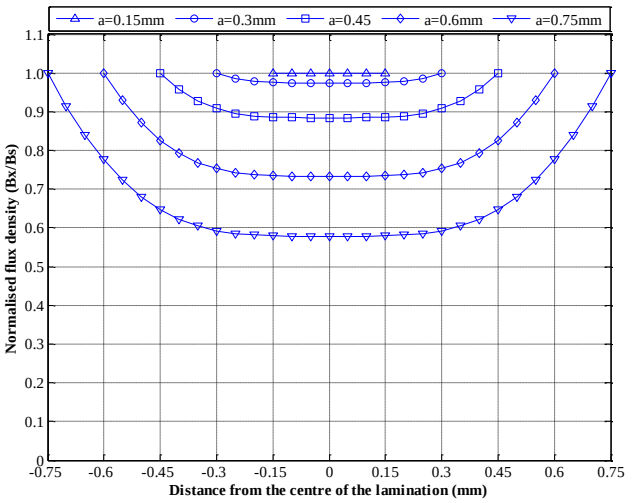

(b)

Fig 18 Normalized flux density penetration into lamination of different thicknesses at frequency of 50 Hz and surface flux density (a) B_s=1.3 T and (b) B_s=1.7 T

Based on FEM modeling and analytical results, it was found that skin effect is a key factor in the eddy current power loss investigation of magnetic cores not only at high frequencies, but also at low frequencies when the core is affected by the edge burrs. The proposed configuration in this Part I paper will be used in Part II paper to estimate eddy current power loss of burr affected magnetic cores in a wide range of magnetising frequency and flux density.

ACKNOWLEDGMENT

The authors are grateful to Cogent Power Ltd. for providing the electrical steel sheets.

REFERENCES

[1] K Lee, J Hong, K Lee, S B Lee and E J Wiedenbrug, "A Stator Core Quality Assessment Technique for Inverter-fed Induction Machines", IEEE Industry Applications Society Annual Meeting, Oct 2008, pp 1-8

[2] M B Aimoniotis and A J Moses, "Evaluation of induced eddy currents in transformer sheets due to edge-burrs, employing computer aided design programs," in Athens Power Tech '93 Proc., 1993, VOL. 2, pp. 847–849

[3] H Hamzehbahmani, A J Moses and F J Anayi "Opportunities and Precautions in Measurement of Power Loss in Electrical Steel Laminations Using the Initial Rate of Rise of Temperature Method" IEEE Trans. Mag. VOL. 49, NO. 3, March 2013, pp 1264- 1273

[4] A J Moses and M Aimoniotis, "Effects of artificial edge burrs on the properties of a model transformer core," Physica Scripta, VOL. 39, 1989, pp. 391–393

[5] R Mazurek, P Marketos, A J Moses and J N Vincent "Effect of artificial burrs on the total power loss of a three-phase transformer core", IEEE Trans. Magn., VOL. 46, NO. 2, 2010, pp.638 -641

[6] BS EN 60740-1:2005 "Laminations for transformers and inductors- Part 1: mechanical and electrical characteristics"

[7] M Lindenmo, A Coombs and D. Snell, "Advantages, properties and types of coatings on non-oriented electrical steels", Journal of Magnetism and Magnetic Materials 215-216 (2000), pp. 79-82

[8] W J Deng, Z C Xie, P L and T K Xu, "Study on Burr Formation at the Top Edge in Rectangular Groove Cutting", Journal of Advances in Materials Science and Engineering, VOL. 2012

[9] C A Schulz, S p Duchesne, D Roger and J N Vincent, "Capacitive Short Circuit Detection In Transformer Core Laminations", Journal of Magnetism and Magnetic Materials 320 (2008) e911–e914

[10] D B Paley "Current Low Power Core Testing Using EL CID" IEEE Colloquium "Understanding your condition monitoring (Ref. No. 1999/117)" April 1999, pp 7/1-7/4

[11] D R Bertenshaw, J F Lau and D J Conley, "Evaluation of EL CID Indications not associated with Stator Core Inter-laminar Insulation Faults" IEEE Electrical Insulation Conference, June 2011, pp 254- 260

[12] D B Paley "Current Low Power Core Testing Using EL CID" IEEE Colloquium "Understanding your condition monitoring (Ref. No. 1999/117)" April 1999, pp 7/1-7/4

[13] C A Schulz, S Duchesne, D Roger and J N Vincent "Short Circuit Current Measurements between Transformer Sheets", IEEE Trans Magn, VOL. 46, NO. 2, Feb 2010, pp 536-539

[14] C A Schulz, D Roger, S Duchesne and J N Vincent, "Experimental Characterization of Interlamination Shorts in Transformer Cores", IEEE Trans Magn, VOL. 46, NO. 2, Feb 2010, 614-617

[15] S B Lee, G Kliman, M Shah, D Kim, T Mall, K Nair and M Lusted, "Experimental Study of Inter-laminar Core Fault Detection Techniques based on Low Flux Core Excitation" IEEE Trans On Energy Convers, VOL. 21, NO. 1, March 2006, pp 85-94

[16] S B Lee, G B Kliman, M R Shah, N K Nair and R M Lusted "An iron core probe based inter-laminar core fault detection technique for generator stator cores" IEEE Trans. Energy Convers., VOL. 20, NO. 2, Jun. 2005, pp. 344–351

[17] S B Lee, G B Kliman, M R Shah, W T Mall, N K Nair and R M Lusted "An advanced technique for detecting inter-laminar stator core faults in large electric machines" IEEE Trans On Industry Applications, VOL. 41, NO. 5, Sep/Oct 2005, pp. 1185–1193

[18] Z Popovic and B D Popovic, "Introductory Electromagnetics", Prentice Hall, 2000.

[19] F Brailsford, "Physical Principles of Magnetism", Van Nostrand, 1966

[20] M. B. Balehosur, Ph. Marketos, Anthony J. Moses and Jean Noél Vincent "Packet-to-Packet Variation of Flux Density in a Three-Phase, Three-Limb Power Transformer Core" IEEE Trans Magn, VOL. 46, NO. 2, February 2010, pp. 642-645

[21] K G Nilanga, B Abeywickrama, T Daszczynski, Y V Serdyuk and S M Gubanski," Determination of Complex Permeability of Silicon Steel for Use in High-Frequency Modeling of Power Transformers", IEEE Trans Magn, VOL. 44, NO. 4, April 2008, pp. 438-444

[22] P Anderson, D R Jones and J Hall, "Measurement of resistivity of soft magnetic laminations at elevated temperatures", Journal of Magnetism and Magnetic Materials, VOL 304, Issue 2, 2006, pp. e546-e548